2nd CIRP Conference on Composite Material Parts Manufacturing

Improved Energy Absorption in 3D Woven Composites by Weave Parameter Manipulation

Geoffrey Neale[a]*, Monali Dahale[a], Sanghyun Yoo[b], Nathalie Toso[b], Cormac McGarrigle[c], John Kelly[a], Edward Archer[a], Alistair McIlhagger[a] and Eileen Harkin-Jones[a]

[a]*Engineering Research Institute, Ulster University, Shore Road, Newtownabbey, BT37 0QB, United Kingdom*
[b]*Institute of Structures and Design, German Aerospace Center (DLR), Stuttgart, Germany*
[c]*Centre for Engineering and Renewable Energy, Ulster University, Magee Campus, BT48 7JL, United Kingdom*

** Corresponding author. E-mail address: neale-g@ulster.ac.uk*

Abstract

3D woven composites show significantly improved out-of-plane properties over traditional 2D laminates. This high through-thickness reinforcement is desirable in crashworthiness applications where crushing energy can be increased by composites' improved interlaminar toughness. However, their use in practical applications is stunted by the poor understanding of how small variations in weave parameters, whether intended or not, affect the performance of these materials. Here, we demonstrate that small changes in textile properties, in this case pick density and float length have a knock-on effect that can greatly improve or diminish the crush performance of a 3D woven layer-to-layer structural fabric. Quasi-static and dynamic energy absorption values up to approximately 95J/g and 92J/g respectively are achieved. Crush performance is investigated on omega-shaped coupons, under both quasi-static and dynamic loading conditions with crush rates between 2mm/min and 8.5m/s. The failure mechanisms present during progressive crush under quasi-static loading transitions between more expected brittle dominated failure and ductile dominated failure, which is more typical of metals under similar loading conditions. Whereas when dynamic loading is considered, the materials present a more typical splaying failure event. As a result, additional exploration of the three-point bending response of these varied architectures is presented as a means of further explaining the interplay between lamina bending and progressive folding/micro-buckling in these materials. The effect of the weave's architectural alterations on physical composite properties such as weight, density and conformability to shape is also investigated.

Peer-review under responsibility of the scientific committee of the 2nd CIRP Conference on Composite Material Parts Manufacturing.

Keywords: 3d wovens; layer-to-layer; energy absorption; pick density; float length.

1. Introduction

Progressive failure in crash structures used in transport vehicles like cars, trains and planes are required to be accurately predictable, requiring either extensive modelling or experimentation [1]. In the case of 3D woven materials, insufficient data exists to accurately model more complicated architectures.

Practically, small variations in the textile architecture can be introduced during weaving which are either intentional (by design) or unintentional (weaving errors). These variations can cause disproportionately large knock-on effects to physical and mechanical composite properties. This is especially true where composite geometries deviate from flat and thin. Changes are caused by variability in yarn stacking, nesting, waviness and crimp and are in most cases are unavoidable but acceptable [2].

This current research focuses on the energy absorption capability or crashworthiness of these 3D composite materials. Crashworthiness describes a structure's ability to absorb energy through progressive failure, whilst maintaining the load profile during the energy absorbing event [3]. This process dictates controlled and predictable failure which progresses down the structure as the crush zone advances. Reference is mostly made to maximising the specific energy absorption (SEA), which is the total area under the load (P) versus displacement (δ) plot expressed in Joules (J), all divided by the mass (M) of the damaged portion of the structure and can be represented by the equation:

Peer-review under responsibility of the scientific committee of the 2nd CIRP Conference on Composite Material Parts Manufacturing.

$$SEA = \frac{\int P \, d\delta}{M} \quad (1)$$

When the SEA of the three fundamental 3D woven architectures (orthogonal, layer-to-layer and angle interlock) are compared, orthogonal architectures generally outperform others in quasi-static crush but layer-to-layer architectures show superior dynamic crush behavior [4]. Additionally, layer-to-layer architectures are substantially more efficient at transferring loading around bends in highly curved architectures [5]. As a result, the baseline architecture selected in this work is a modified layer-to-layer configuration.

There is a general dissimilarity between the expected progressive failure modes in 2D laminates and 3D wovens. This is due to the dissimilarity between the level of homogeneity in the different materials [4,6]. However, the SEA in 3D woven composites has been shown to range from parity with, to moderately exceeding, the SEA in equivalent 2D laminates [4].

Although there is a significant body of literature on similar open section 2D composites such as in Jackson et al. [3], Feraboli et al. [7] and David et al. [8], little has been explored in the realm of crashworthy 3D woven composites. Goering et al. [4] published a limited but important work focused on crashworthiness of orthogonal weaves. But no work has explored the effect of parameter modifications on crashworthiness within a 3D architecture. Dahale et al. [9] explored the effect of pick (weft yarns) density on warp direction mechanical properties. Pick density, that is the number of weft (transverse) yarns per centimetre, has been shown to improve in-plane warp direction properties in layer-to-layer composites. The authors are currently working on a similar investigation into warp binder float length, as this has been shown by Dai et al. [2] to affect in-plane properties in orthogonal architectures. From a textile perspective, longer float is known to improve tear resistance and drape, but can encourage large amounts of yarn slippage [10].

This research investigates how small intentional modifications to both pick density and float length affect the manufacture, conformability and crush energy absorption of 3D layer to layer composites. The key point here is that these changes can be accomplished without significant changes to the fabric design/manufacture process but can produce highly desirable results. The compression and flexural response of the architectures is also explored in an effort explain the intricacies of the progressive failure behaviour exhibited by these materials but is not the main focus of the research.

2. Materials and Methods

2.1. Manufacture

A modified 3D woven layer-to-layer type baseline architecture (BA) was designed which consisted three warp layers, four weft layers and three warp binder yarns. The fabric architecture is graphically explained in Figure 1 (left) where the binder yarns (blue) connect the weft yarns (white) immediately above and below each warp yarn (red). The BA architecture was then altered by changing the pick density and the binder float length. The full list of fabric preform parameters is listed in Table 1 and the changes are graphically represented in Figure 1. The pick density was increased from 10 wefts/cm or 2.5 wefts/cm/layer (BA) to 16 wefts/cm or 4 wefts/cm/layer (WD) while the float length was kept constant at 1 weft. The binder float length was then increased to 2 wefts (FL) with a constant pick density of 16 picks/cm. All 3D woven fibre preforms were made on a Jacquard loom from Toray T700-50C (12k yarns) carbon. The finished preforms were then infused with PRIME 20LV epoxy resin via RTM and cured at 50°C for 16 hours

Table 1: 3D woven preform fabric characteristics.

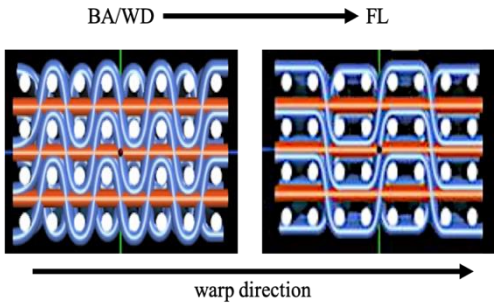

Figure 1: Comparison between weave architectures in BA/WD specimens and FL specimens.

Specimen Type	Pick Density (wefts/cm)	Binder Float (wefts)	Yarn Content (%) [warp/weft/binder]	Yarn Crimp (%) [warp/weft]
BA	10	1	27 / 46 / 27	3.7 / 1.4
WD	16	1	21 / 58 / 21	2.8 / 1.3
FL	16	2	21 / 58 / 21	1.3 / 1.2

*All architectures have constant warp (end) density of 12 wefts/cm

The omega-shaped specimen geometry was picked for its ease of manufacture and stability in lieu of an accepted standard for crush testing [7]. The shape is based on work by DLR [8] and is shown in Figure 2a. The specimens were 60±2mm and 90±2mm long for quasi-static and dynamic specimens respectively, both with a thickness of 2.5±0.5mm. A saw tooth shaped trigger was machined into the leading edge of the specimen to initiate progressive crush (Figure 2b). The specimens were then set in a 10mm deep aluminium base to secure them during testing.

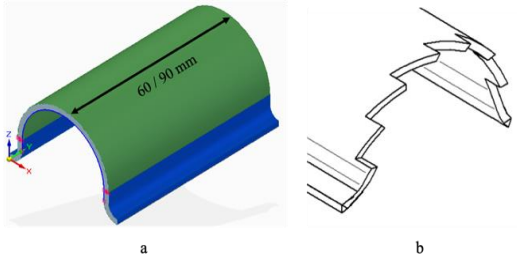

Figure 2: (a) Omega-shaped specimen (b) saw-tooth trigger

2.2. Crush Testing

Specimens were crushed quasi-statically in a uniaxial compression mode between two metal platens in an Instron electromechanical Universal Testing System (5500R), with a 100kN load cell. Quasi-static tests were initiated at a crosshead displacement speed of 2mm/min for the first 15mm of crush which was then increased to 20mm/min up to 40mm maximum crosshead displacement (see crosshead velocity in Figure 4**Error! Reference source not found.**). Dynamic specimens were crushed in an Instron VHS-100/20 with a 100kN load cell, with an average impact velocity of 8.5m/s up to 60mm maximum displacement. Four of each iteration were tested quasi-statically and three of each were tested dynamically.

2.3. Flexural Testing and Compression Testing

Specimens were tested in a three-point bending configuration in accordance with ASTM D7264 to derive flexural properties. The test was stopped once a 20% stress drop was noted in the stress-strain response. Five specimens are tested in the warp direction only. For compressive analysis, specimens were tested in accordance with the Boeing-modified ASTM D695 standard, while being compressed in an anti-buckling jig. Both tests were carried out on an Instron Universal Testing System (5500R), with a 100kN load cell. Five specimens are tested in the warp direction only.

3. Results & Discussion

3.1. Fabric Conformability

How 3D fabrics conform to a desired geometry is an important consideration in its suitability for purpose. The conformability of 3D woven fabrics can be a complicated parameter to investigate as the geometry strongly affects the yarn nesting, tow misalignment and yarn stacking which can all affect local mechanical properties.

When discussing the conformability of 3D fabrics for such highly curved architectures, the main characteristics investigated here are:

1. Yarn Stacking/Nesting (out-of-plane alignment) – the nesting behaviour in yarns;
2. Tow misalignment (in-plane misalignment) – the in-plane deviation of the yarn system from the ideal.

Table 2: Fabric Compressibility analysis.

Specimen Type	Fabric Thickness (mm)	Areal weight (kg/m^2)	Unit Cell Size warp/weft (mm)	Composite Thickness (mm)	v_f warp (%)	v_f weft (%)
BA	2.9	1.5	12/12	2.5	44	40
WD	4.2	2.2	7/12	2.9	44	53
FL	3.8	2.4	14/12	3.0	44	53

In BA specimens, the more perfect stacking of warp and binder yarns (Figure 3b) leaves empty spaces between them which become resin rich regions upon consolidation. There are generally straight columns of yarn stacks, which only tend to deviate near the tight curve in the flange, in BA and FL specimens show in in Figure 3b and c. This can be a problem in tension loading where the collimation of warp tows could result in uncontrolled binder tow tension [6], however this doesn't affect this compressive loading scenario in the same way. This is stacking is desirable because the practical architecture would match that of an equivalent model and allow more accurate failure prediction. Additionally, the lack of slanting of the yarn/binder columns suggests good axial alignment of those yarns and hence better failure performance in compression [11] and crush [3].

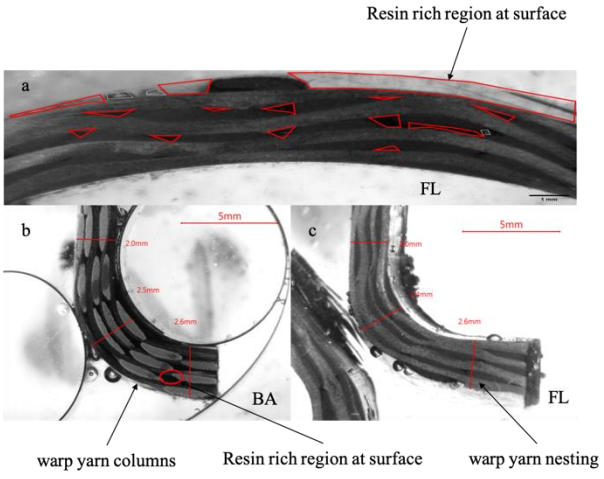

Figure 3 : Micrographs of bend radii in omega-shaped specimens: (a)semi-circle in FL; (b) flange in BA; and (c) flange in FL

There is visible nesting present in WD and FL specimens where warp and binder yarns slide along the cross-section to achieve the same thickness as in BA specimens. In thicker fabrics (WD and FL), there is pinching at the corners of the mould which cause a thinning of the fabric at the semi-circle of the omega-shape. As a result, the of percentage resin rich regions increases from 5% in BA to 10% in the curved section of WD and FL specimens. This is caused by a thin surface layer of resin that forms on the outer edge of the curved section (maximum 0.3 mm thickness). This hasn't been shown to provide any instability in crushing carried out later in this paper and all specimens crush progressively.

To investigate the effect of conformance to the omega-shape on the in-plane alignment of yarns, coloured yarns are incorporated into the preform that follow the paths of the weft and binder yarns. Tracking the warp yarns from the surface is not possible since, in this architecture, warp yarns do to ever run along the surface of the material, but we can assume the have similar in-plane paths to that of the binders. WD and FL preforms show very little (less than 2°) noticeable in-plane deviation in either the binder or weft tows. However, there is visible deviation (average 8°) of the weft tows in BA specimens from their straight path. WD and BA preforms have a higher pick density than BA preforms, and it is this increased yarn packing that resists in-plane tow movement caused by drape more strongly.

At internal bend radii, weft yarns wrinkle nearer the centre of curvature and warp and binder yarns bunch together. At external bend radii, weft yarns straighten out and stretch to

bridge the gap caused by the spacing out of warp and binder yarns. These phenomena are consistently observed throughout all specimens but is less so pronounced in WD specimens. The pick density and number of binding points affects the bending rigidity in a given orientation. In future, these researchers intend to use this knowledge about conformability and that of the material's crashworthiness performance to design fabric architectures which would then more heavily account for the desired geometry and remove "defects" like improper yarn stacking and tow misalignment.

3.2. Effect of Pick Density on Quasi-static SEA

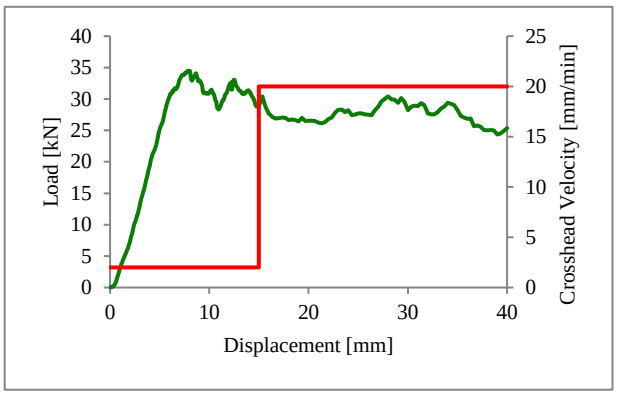

Figure 4: Typical load displacement curve showing quasi-static crush in a WD specimen.

The crushing results for all specimens are presented in Table 3 and Figure 6. A typical progressive load-displacement curve is shown in Figure 4.BA and WD specimens fail via events in which progressive folding plays a major role. This is uncommon in 2D laminates and in 3D composites [4], which usually fail via splaying, brittle fracture or fragmentation as defined by Farley et al. [12] and Hull et al. [13]. Splaying dictates the splitting of the laminate down a central delamination crack leading to the formation of inward and outward fronds, whereas fragmentation is an even higher energy progressive failure event in which the material is almost pulverized into particles smaller than the thickness of the laminate. Brittle fracture is a combination of those two previously mentioned failures, with pulverisation of the inner layers and splaying of the outer ones.

Folding in 3D wovens is possible and initiates because of the high out of plane deviation of load carrying (warp) yarns, which converts some in-plane stress flow to out-of-plane stresses. During folding, local buckling allows the material to fold over and maintain loading through flexural resistance [13]. BA specimens exhibit mixed-mode failure which is initiated by splaying during the initial trigger phase but then transitions to folding post triggering (Figure 5a). WD specimens fail almost exclusively by progressive folding from the onset of crush. In both cases, failure initiates at the flanges. This propagates into a circumferential crack in the weft direction around the curved section of the specimen which then serves as a hinge point for a local folding event (Figure 5b).

Flexural and compressive properties are provided in Table 4. In BA specimens where compressive strength is 11% lower and characterised by brooming failure. When the crush front reaches that circumferential brooming crack, external yarns which have already broomed outwards continue to splay while internal yarns fold and push splaying fronds outward. In WD specimens the material has a 42% smaller warp direction unit cell which increases the compressive strength by 11% in the warp direction fails in compression through thickness shear. [9]. The lack of broomed material allows for a more cohesive hinge point and purer progressive folding. Increases in compressive strength with pick density improve buckling resistance and hence a 16% higher initial load (F_{max}) and a 5% higher SEA.

Improvements are also the result of improved flexural rigidity. WD specimens have a 40% higher flexural stiffness and 36% higher flexural strength than in BA specimens (Table 4) and can better resist folding. This is because initial flexural failure is fibre-dominated in WD specimens with tow rupture (tensile zone) and though thickness shear (compression zone), rather than by matrix cracking and pull-out in BA specimens.

However, as seen in 2D laminates [14], this folding only event in WD specimens is not as efficient as crushing events with other more brittle failure mechanisms, which is supported by its 10% lower Crush Force Efficiency (CFE) than in BA

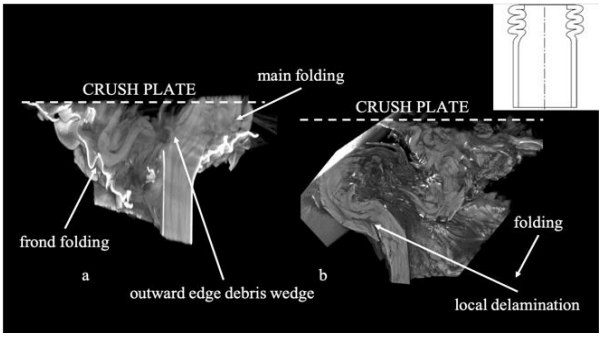

Figure 5: Micro-CT images showing cross-section view of progressive folding events in (a) BA and (b) WD specimens.

Table 3: Crushing test results.

Specimen	Mass per mm of crush (g/mm)	F_{max} (kN)	Favg (kN)	SEA (J/g)	SEA per mm crush (J/g mm)	CFE (%)
BA	0.297	28.8 [6.9]	27.6 [0.9]	84.2 [2.5]	2.4 [2.5]	96.4 [6.3]
BA-DYN		23.9 [3.9]	20.5 [5.2]	70.1 [8.1]	1.3 [8.1]	85.9 [1.4]
WD	0.290	33.3 [3.3]	27.5 [4.3]	88.5 [1.4]	2.5 [1.4]	82.5 [2.2]
WD-DYN		28.6 [0.0]	26.6 [1.9]	92.9 [4.6]	1.7 [4.6]	93.0 [1.9]
FL	0.335	28.8 [2.6]	24.3 [5.6]	65.1 [12.4]	1.9 [12.4]	84.3 [4.9]
FL-DYN		26.0 [4.1]	25.0 [2.5]	77.0 [5.4]	1.4 [5.4]	96.5 [2.3]

*Coefficient of variation indicated in parenthesis

specimens and only a small SEA increase. This is because a much higher F_{max} but more or less the same average sustained loads (F_{avg})

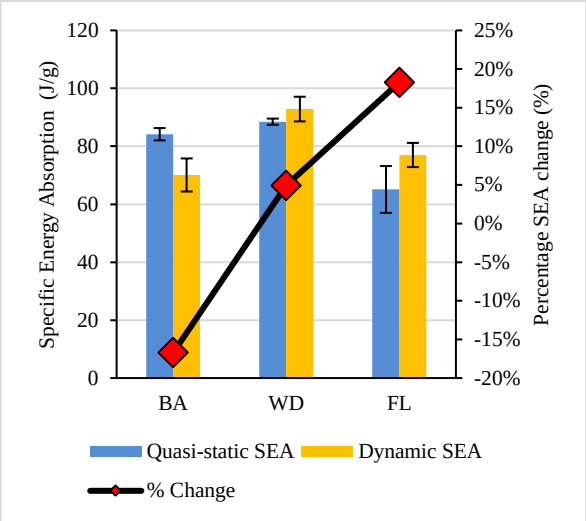

Figure 6: SEA characteristics of crushed specimens.

These improvements are accomplished without any addition of axial reinforcement and negligible change in the mass per unit crush. The use of v_f as a metric in this analysis is misleading since it varies at different points in the geometry. Additionally, the v_f the warp direction is fixed (Table 2) but changes significantly in the weft direction; this direction is not tested in crushing. In the literature mass per unit mm has been used as a much more effective metric [3].

Table 4: Flexural and compressive properties.

Specimen Type	Flexural Strength (MPa)	Flexural Modulus (GPa)	Compressive Strength (MPa)
BA	372 [59.3]	20 [0.6]	307 [20.9]
WD	504 [49.4]	28 [2.3]	344 [54.9]
FL	320 [25.8]	32 [2.6]	-

*Standard deviation indicated in parentheses

3.3. Effect of Float Length on SEA

Increasing the float makes the fabric more unstable and as a result, it must be woven more densely to counter this i.e. a higher pick density is needed [10]. Comparisons between FL and WD specimens are made because both materials have the same pick density (Table 2).

FL specimens exhibit a 27% decrease in quasi-static (Figure 6) alongside no real change in CFE compared to WD. This is because FL specimens have fewer binding points per unit length (larger unit cell (Table 2)) than WD and so have a lesser bending rigidity to support folding, evidenced by its 37% lower flexural strength. Dahale et al. [9] showed that a larger unit cell in layer to layer 3D woven composites decreases the compressive strength of the material. This manifests itself as a 13% lower F_{avg} in FL specimens.

The flexural modulus in FL specimens is 14% higher than in WD specimens (Table 4). This is expected as FL specimens have the lowest crimp, which has a strong influence on modulus [11]. Lower failure strain and strength results in sharper bend angles during folding where yarns just fracture completely and no longer maintain loading (Figure 7). This, along with an increased mass per unit crush length compared to WD (Table 3), is responsible for the lower SEA of the material compared to WD and BA.

When crush failure is observed, there seems to be a significant amount of external yarn dislodgement which then allows internal yarns to fold (Figure 7). External weft yarns are less constrained in FL specimens than in WD ones and the through thickness stresses simply dislodge them during folding (quasi-static) or splaying (dynamic).

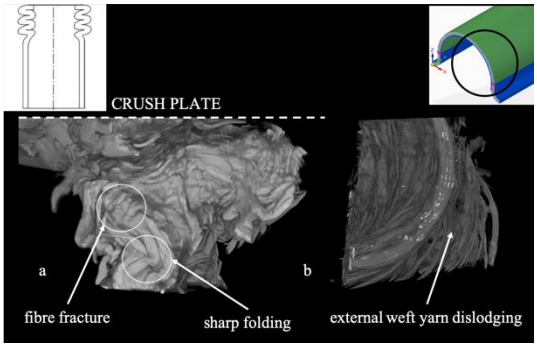

Figure 7: Micro-CT images showing a cross-section view of (a) progressive folding and (b) external yarn slippage in FL specimens.

3.4. Dynamic versus Quasi-static Performance

All three dynamically tested specimen types (BA-DYN, WD-DYN and FL-DYN) fail via splaying which results in inward and outward frond formation. There is significantly less axial tearing and circumferential cracking in WD-DYN specimens than in BA-DYN ones. Greater hoop reinforcement (higher pick density) in WD-DYN specimens results in lower individual yarn hoop stresses during the splaying event, less weft yarn fracture yarns and hence fewer fronds. The more rigid and larger fronds in WD-DYN specimens can sustain higher loads through bending resistance of the frond material. In FL specimens, additional energy is dissipated through the debonding and ejection of complete weft yarns at the outer surface of the curve (Figure 7b). However, this reduces the rigidity of fronds and results in a lower SEA than in WD specimens.

Quasi-static and dynamic SEA values for each specimen type are compared. WD-DYN and FL-DYN specimens show an increase in SEA of +5% in WD and +18% respectively. This is uncommon in crashworthiness studies in both 2D and some types of 3D composites, where diminished dynamic energy absorption is observed compared to quasi-static energy absorption [4]. This because of matrix dominated failure and matrix embrittlement at higher strain rates i.e. easier cracking and less SEA [3,4]. Folding in composites is known to be inefficient [13,15]. Just by virtue of the transition from folding to splaying (higher energy) between the quasi-static and dynamic regimes, a higher SEA is expected. Additionally, in WD-DYN and FL-DYN specimens, failure is fibre- dominated

(frond bending and binder fracture), which is not true for BA-DYN specimens which has lesser binding points and less frond rigidity.

Some 3D woven composites are known to show improved mechanical performance as the strain rate increases [16–18]. Through thickness load transfer and load transfer between fibre and matrix is generally quite good in 3D composites and increases with increased binding. It is worth noting that every 3D textile explored in the literature is different and cannot be directly compared. However, this work shows a good representation of the improvement of performance with increasing strain rate, particularly in FL and WD specimens.

4. Conclusions

- Fabric preform conformability to shape is generally good with only minor deviations of the out-of-plane yarn stacks from the ideal at tight bend radii. In-plane yarn alignment is good but is worst in BA fabrics where the looser structure allows for greater deviation of the weft yarns.
- Increasing pick density and float length from the baseline showed a general decrease in quasi-static CFE (higher F_{max} brought on by increased compressive strength) but an increase in dynamic CFE (higher F_{avg} brought on by greater binder turns and improved splaying).
- Higher pick density and float length provided more significant increases to the dynamic SEA of the composite. FL and WD specimen SEA values are 10% and 33% up from the values in BA specimens.
- Float length increase provides a 18% increase in dynamic SEA compared to quasi-static SEA, and in general, both changes (pick density and float length changes) have a positive effect on that percentage change value, pushing them into the positive region which is not reported in 2D laminates.

In future, the authors hope to more closely investigate the interplay between the fabric conformability and the material's ability to absorb energy. In that, novel architectures that are designed specifically for the geometry and function can be realized.

Acknowledgements

This work was supported by EU Horizon 2020 Marie Skłodowska-Curie Actions Innovative Training Network-ICONIC [grant agreement number: 721256]. The authors acknowledge the support from The Engineering Research Centre (ECRE) of Ulster University and Axis Composites Ltd, especially Roy Brelsford, Dr Glenda Stewart, Simon Hodge and Graeme Craig.

References

[1] M. Carruth, Design Optimization Case Study: Car Structures, 2011. http://lcmp.eng.cam.ac.uk/wp-content/uploads/W6-Design-Optimization-Case-Study-Car-Structures.pdf.

[2] S. Dai, P.R. Cunningham, S. Marshall, C. Silva, Influence of fibre architecture on the tensile, compressive and flexural behaviour of 3D woven composites, Compos. Part A Appl. Sci. Manuf. 69 (2015) 195–207. doi:10.1016/j.compositesa.2014.11.012.

[3] A. Jackson, S. Dutton, A.J. Gunnion, D. Kelly, Investigation into laminate design of open carbon-fibre/epoxy sections by quasi-static and dynamic crushing, Compos. Struct. 93 (2011) 2646–2654. doi:10.1016/j.compstruct.2011.04.032.

[4] J. Goering, H. Bayraktar, 3D Woven Composites for Energy Absorption Applications, in: SPE Automot., 2016: pp. 1–18. doi:10.4271/2016-01-0530.

[5] M.N. Saleh, C. Soutis, Recent advancements in mechanical characterisation of 3D woven composites, Mech. Adv. Mater. Mod. Process. 3 (2017) 12. doi:10.1186/s40759-017-0027-z.

[6] J.P. Quinn, A.T. McIlhagger, R. McIlhagger, Examination of the failure of 3D woven composites, Compos. Part A Appl. Sci. Manuf. 39 (2008) 273–283. doi:10.1016/j.compositesa.2007.10.012.

[7] P. Feraboli, F. Deleo, F. Garattoni, Efforts in the standardization of composite materials crashworthiness energy absorption, Proc. 22nd ASC Tech. Conf. Seattle, WA Sept. (2007) 17–20.

[8] M. David, A.F. Johnson, H. Voggenreiter, Analysis of Crushing Response of Composite Crashworthy Structures, Appl. Compos. Mater. 20 (2013) 773–787. doi:10.1007/s10443-012-9301-8.

[9] M. Dahale, G. Neale, R. Lupicini, L. Cascone, C. McGarrigle, J. Kelly, E. Archer, E. Harkin-Jones, A. McIlhagger, Effect of weave parameters on the mechanical properties of 3D woven glass composites, Compos. Struct. 223 (2019) 110947. doi:10.1016/j.compstruct.2019.110947.

[10] L. Thomas, Woven structures and their impact on the function and performance of smart clothing, Woodhead Publishing Limited, 2009. doi:10.1533/9781845695668.2.131.

[11] F. Stig, S. Hallström, Influence of crimp on 3D-woven fibre reinforced composites, Compos. Struct. 95 (2013) 114–122. doi:10.1016/j.compstruct.2012.07.022.

[12] G.L. Farley, Energy Absorption of Composite Materials, J. Compos. Mater. 17 (1983) 267–279. doi:10.1177/002199838301700307.

[13] D. Hull, A unified approach to progressive crushing of fibre-reinforced composite tubes, Compos. Sci. Technol. 40 (1991) 377–421. doi:10.1016/0266-3538(91)90031-J.

[14] C. Priem, R. Othman, P. Rozycki, D. Guillon, Experimental investigation of the crash energy absorption of 2.5D-braided thermoplastic composite tubes, Compos. Struct. 116 (2014) 814–826. doi:10.1016/j.compstruct.2014.05.037.

[15] G.L. Farley, R.M. Jones, Energy Absorption Capability of Composite Tubes and Beams, Hampton, Virginia, 1989. http://www.dtic.mil/dtic/tr/fulltext/u2/a233515.pdf (accessed February 3, 2017).

[16] B. Sun, B. Gu, Shear behavior of 3D orthogonal woven fabric composites under high strain rates, J. Reinf. Plast. Compos. 25 (2006) 1833–1845. doi:10.1177/0731684406068452.

[17] J. Zhao, L. Zhang, L. Guo, Y. Yang, Dynamic properties and strain rate effect of 3D angle-interlock carbon/epoxy woven composites, J. Reinf. Plast. Compos. 36 (2017) 1531–1541. doi:10.1177/0731684417715712.

[18] R. Gerlach, C.R. Siviour, J. Wiegand, N. Petrinic, In-plane and through-thickness properties, failure modes, damage and delamination in 3D woven carbon fibre composites subjected to impact loading, Compos. Sci. Technol. 72 (2012) 397–411. doi:10.1016/j.compscitech.2011.11.032.